PHYSICAL AND MECHANICAL PROPERTIES OF THE ROTOKAWA ANDESITE FROM PRODUCTION WELLS RK 27_L2, RK 28 AND RK 30

Paul A. Siratovich[1], Jonathan Davidson[1], Marlene Villeneuve[1], Darren Gravley[1], Ben Kennedy[1], Jim Cole[1], Latasha Wyering[1], and Linda Price[2]

[1]University of Canterbury Department of Geological Sciences. Private Bag 4800, Christchurch, NZ, 8041

[2] Mighty River Power Company Ltd., 283 Vaughan Rd, Rotorua, NZ, 3040

paul.siratovich@gmail.com

Keywords: *Rotokawa, mechanical, properties, physical, acoustic, andesite, production, strength, tensile, petrology, alteration*

ABSTRACT

Mighty River Power's geothermal production wells of RK 27_L2, RK 28 and RK 30 were spot cored within the Rotokawa Andesite during the drilling of the wells. Core recovery was nearly 100% from the three cores and these were analyzed and logged by GNS Science at Wairakei Research Centre. Subsequently, the cores were transferred to the University of Canterbury to determine alteration mineralogy and physical properties, and were subjected to rigorous mechanical testing to determine strength and stiffness properties. The Rotokawa Andesite ranges from mildly altered andesite lavas and breccias to a complete replacement by alteration products where host fabric can no longer be easily identified. Density, porosity, and acoustic velocity measurement were measured and samples were subjected to strength testing including uniaxial compressive strength and Brazilian tensile strength. Results are presented here with preliminary correlations between results of mechanical strength testing to physical parameters.

1. INTRODUCTION

Physical properties of the host rocks of geothermal reservoirs are of extreme importance to designing and implementing energy production from these resources. A full-scale knowledge of rock properties allows reservoir fluid-flow models, drilling optimization, reservoir management, reservoir capacity and many other factors to be modeled and predicted over the usable life of a geothermal system. However, these properties can be very difficult to ascertain during drilling and completion operations. This can be attributed to drilling characteristics of the productive zones of the reservoir. During the drilling of many geothermal wells, reservoir intervals often have to be drilled 'blind'; without circulation of cuttings to surface. This poses a problem for determining the lithology and alteration state of the host reservoir rocks. Therefore, it is often prudent to drill spot cores from the reservoir rocks that can be used to study and determine reservoir physical, mechanical and thermal properties.

This study provides the initial results of a detailed analysis of spot core obtained from wells RK 27_L2, RK 28 and RK 30, drilled within the Rotokawa Andesite. Initial testing characterized the properties of porosity, bulk density, acoustic velocities, uniaxial compressive strength (UCS), and Brazilian indirect tensile strength. When the cores were obtained by Mighty River Power (MRP) and subsequently analyzed at GNS Science (GNS, 2009 and 2010) only selected samples were subjected to such rigorous analysis. This study complements the initial work and goes on to provide a detailed analysis of each competent (whole) section of core obtained from the drilling. It is the start of a long-term investigation based at the University of Canterbury (UC) to establish a full characterization of geothermal reservoir rock properties that will focus on engineering challenges such as; drilling optimization relating to alteration, fracture stimulation, and reservoir stress state characterization. By establishing benchmark values such as those presented in this study, comparisons can be drawn between samples that will undergo further stressing and testing in the laboratory.

2. ROTOKAWA GEOTHERMAL FIELD

2.1 Rotokawa Geothermal Field

The Rotokawa Geothermal Field is host to a high-enthalpy, two-phase steam field operated by Mighty River Power Limited. The field is located approximately 14 kilometers north-east from the city of Taupo, New Zealand. Rotokawa is being sourced to provide working fluids to the 34 MWe Rotokawa I and 140 MWe Nga Awa Purua (NAP) power stations (Legmann and Sullivan, 2003 and Horie and Muto, 2010). The two-phase fluid that is sourced from the field at Rotokawa is highly energetic and has an enthalpy of 1,560 kJ/kg. NAP houses the largest single geothermal turbine in the world and is capable of meeting nearly 3% of New Zealand's annual energy consumption.

2.2 Stratigraphy of the Rotokawa Field

The Rotokawa Geothermal reservoir is hosted within the Rotokawa Andesites, a series of lavas, pseudo breccias and breccias. These rocks show intrinsically low permeabilities and the reservoir is mainly composed of fracture networks within the system (Barton et al., 1995; Hickman et al., 1998; Rae, 2007). The andesite overlays bedrock comprised of Miocene 'greywacke'. Overlying the andesite is a sequence of both volcaniclastic and sedimentary units that consist of: Reporoa Group, Wairakei Ignimbrite, Waiora Formation and Huka Falls Formation (Krupp and Seward, 1987 and Rae, 2007).

2.3 Rotokawa Andesite

The Rotokawa Andesite is the host rock for the geothermal reservoir at the Rotokawa Geothermal Field. It consists of massive and flow-banded porphyritic lavas and breccias. Phenocrysts of plagioclase feldspar are abundant as well as

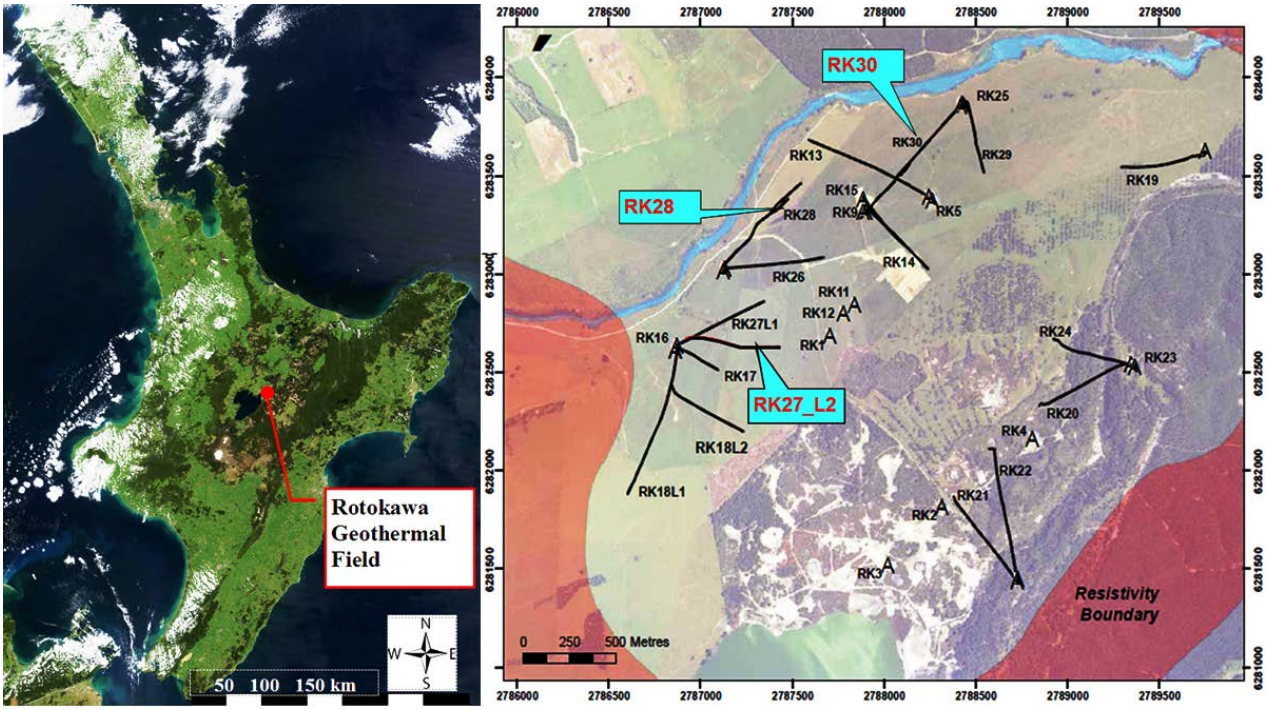

Figure 1: North Island, New Zealand and Rotokawa Geothermal Field. Locations of wells from which core was taken for this study are highlighted. (Modified after Ramirez and Hitchcock, 2010).

pyroxenes in a fine groundmass of plagioclase microlites and magnetites, occasional tuffs and greywacke lithics are observed (Rae, 2007 and Rae et. al, 2010). The andesite is gray to green and occasionally purple in color, depending on alteration within the reservoir. Alteration intensity appears to be less in the lava facies and more intense in the breccia and pseudo-breccia portions of the reservoir (Ramirez and Hitchcock, 2010). In addition to the original porphyritic nature of the andesite, veins of quartz, calcite, anhydrite and epidote are present. Vugs and amygdales within the sample are often filled with chlorite, calcite, hematite, pyrite and chalcedony and are often bounded by quartz rims

3. ANALYSIS AND TESTING METHODOLOGY

Physical and strength characterization was undertaken according to International Society for Rock Mechanics (ISRM) suggested methods for laboratory testing and allow conformable, correlative results to be related to other fields and sample datasets.

3.1 Sample Preparation, Density and Porosity Measurements

Cores were obtained from storage at MRP's Nga Awa Purua power station and brought to UC for further preparation. From the original core taken to UC, 95 specimens were prepared using the following method: each length of component rock was cut into 100mm lengths and overcored using a 40mm diamond core bit, each section of core yielded 2-3 specimens per 100 mm. These samples were then polished to within 0.02 mm of square and had a final length to diameter ratio of 2.0-2.5:1 (ATSM, 2007). Specimens were then dried to 105°C and weighed using saturation and buoyancy techniques. Subsequently, the specimens were water saturated at 20°C under a vacuum of 600 Torr and re-weighed while fully saturated (Ulusay and Hudson, 2007). This allowed for bulk density, particle density and open porosity values to be calculated.

3.2 Thin Section Analysis

Petrology of the core samples was limited to transmitted light microscopy. Samples were described in terms of lithology, apparent primary mineralogy, secondary alteration mineralogy and intensity of alteration. Additionally, alteration indexes (Kilic, R., 1999 and Pochee, 2010) were applied to the samples to give a qualitative description to the severity of alteration within the sample for correlation with additional studies and parameters observed within this study.

3.3 Characterization of P and S Wave Velocities

Compressional (P) and shear (S) wave velocities were measured through the specimens using a GTCS ultrasonic sampling device. The specimens were placed in the Controls 1500 kN uni-axial loading frame and loaded to 10-15 kN. The ends were treated with petroleum jelly to enhance and normalize the contact surface of the acoustic platens (Ulusay and Hudson, 2007). Ultrasonic waves were then shot through the samples and recorded by receivers within the platens. 108 cycles of emissions were shot through each specimen to account for residual noise or boundary effects. The arrival times of the P and S waves were then calculated based on the first arrival of the waveform within the GTCS software by the researcher selecting the exact time of wave arrival time, additionally, the GTCS software can provide researchers with an estimate of elastic modulii, but these were eschewed in favor of results from UCS tests.

3.4 UCS Testing

Specimens were cleaned, dried and fixed with 20mm strain gauges affixed with glue to the sample and ensured to be perpendicular to their respective axes of measurement. Two vertical gauges measured axial strain and two laterally oriented gauges measured radial strain during deformation. Specimens were deformed so that failure occurred within 10-15 minutes of loading (Ulusay and Hudson, 2007). Failure in all cases was catastrophic with each sample displaying total failure. Stress-strain curves were generated from these tests and used to calculate the static Poisson's ratio, Young's modulus, and Bulk modulus using the tangent deformation modulus at 50% of the maximum peak stress.

3.5 Brazilian Tensile Strength Testing

Discs for Brazilian tensile strength testing were cut from core of NX diameter (54mm) 12 individual specimens were tested (4 from each well) in the Controls 1500 kN Uniaxial loading frame. Samples were taped with 1 layer of masking tape and loaded circumferentially with curved loading jaws. Specimens were then loaded to failure so that yield occurred within 2-4 minutes (Ulusay and Hudson, 2007).

4. RESULTS AND DISCUSSION

4.1 Dataset Petrology

We observe the Rotokawa Andesite to be a weakly porphyritic series of lavas, breccias and pseudo-breccias. We also observe both massive and flow-banded lava units with rare expressions of tuff that are almost 100% altered. Alteration in the andesite is pervasive and original mineral assemblages are typically totally replaced by secondary hydrothermal alteration species. Alteration intensity within the sample set is mild to intense with some specimens showing very high porosity and very little original mineralogical texture. Nominal alteration within the dataset appears to be moderate to high in intensity with most original textures preserved but primary mineralogies replaced by secondary mineralogy assemblages.

Within the samples, plagioclase feldspars have been altered to albite, adularia, occasional calcite and rare pyrite. Ferromagnesian minerals have been replaced by chlorite, quartz, calcite and occasional epidote. Vugs within the sample are rimmed by quartz and filled by chlorite. We observe occasional veining in the samples filled with calcite and occasional chlorite and possibly biotite. Microfractured phenocrysts (Figure 2) are abundant in the samples with many relict phenocrysts retaining original texture but replaced by secondary mineralization.

The presence of microfractures in the samples is a key finding as this appears to play an important role in the overall strength of the specimens observed. Microfractures are readily visible under observation and show alteration mineralogies that indicate that these microfractures may have been conductive pathways for fluid migration. Within the microfractures, we typically observe chlorite, calcite and quartz as alteration mineralogies with occasional epidote centers within the fractures.

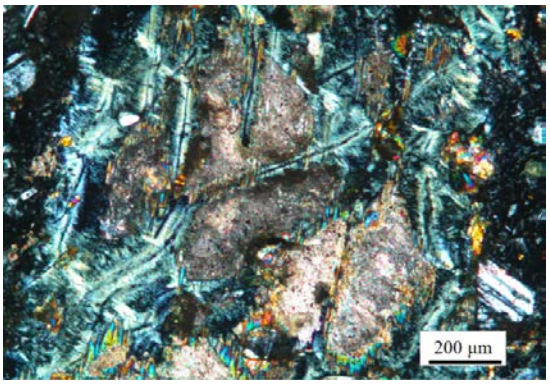

Figure 2. Photomicrograph of thin section sourced from RK30 at 2322.4 mRL. Image shows relict plagioclase phenocryst with pervasive microfracturing. Secondary minerals consist of: chlorite, epidote, calcite, quartz and possible biotite.

4.2 Acoustic Velocities

Acoustic wave attenuation within the samples shows a somewhat linear correlation with density and porosity of the samples, but there are several data-points that do not fit within this correlation. We therefore infer that acoustic velocities must be influenced by the presence of microfractures in the specimens. From this conclusion, acoustic velocities become a useful tool in qualitatively assessing the natural fracture intensity of the samples (Maji, 1995). Natural fracturing within the sample will not only slow acoustic waves but will also yield a much lower average compressive strength for the samples (Lebedev et al., 2003).

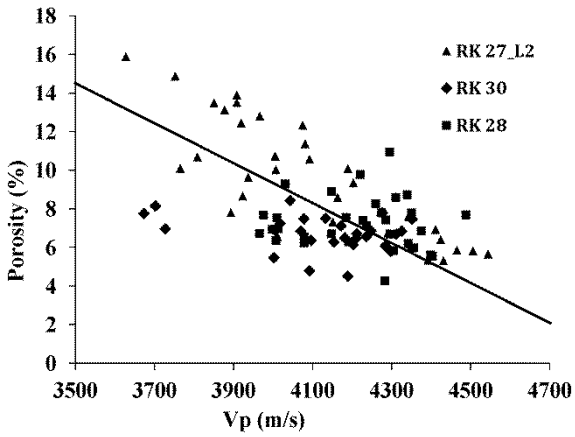

Figure 3: Compressional (P) wave velocities plotted versus porosity. The linear trend shows that as porosity decreases in samples, compressional velocity increases.

Several samples have the same porosity value (7% for instance) but have a wide range of acoustic velocities (Figure 3). This may be due to the fact that the porosity distribution within the samples is anisotropic and waves are attenuated at differing heights in the sample or, this can be attributed to microfractures. Density also affects acoustic velocities, but in the case of similar densities (Figure 4) it is likely that the samples with lower acoustic velocities contain larger concentrations of microfractures that attenuate the propagation of sound waves through the medium.

Table 1: Dimensions, Density, Porosity, UCS and Dynamic Modulii for samples tested in this study

Sample No	*Dimensions (mm)* *H*Ø*	*Density* *(g/cm^3)*	*Porosity* *(%)*	*UCS* *(MPa)*	*Young's Modulus (E)* *(GPa)*	*Poisson' Ratio (ν)*	*Bulk Modulus (G)* *(GPa)*
RK27_L2_2121.5B	93.4 x 38.9	2.44	10.72	85.99	19.9	0.24	13.0
RK27_L2_2121.8A	92.7 x 39.2	2.33	13.49	79.91	25.2	0.26	17.2
RK27_L2_2123.2A	86.4 x 39.2	2.56	6.61	105.26	31.2	0.19	16.6
RK27_L2_2120.4B	88.3 x 39.5	2.56	5.82	211.05	37.7	0.25	24.9
RK27_L2_2121.1C	90.4 x 39.1	2.37	13.10	70.89	21.5	0.18	11.2
RK_28_2310.6A	94.7 x 39.5	2.51	5.85	92.07	19.6	0.09	8.1
RK_28_2310.6C	92.6 x 39.6	2.50	5.97	146.20	43.7	0.27	31.6
RK_28_2310.8C	88.1 x 39.4	2.53	6.72	109.89	27.2	0.34	27.8
RK_28_2310.9B	83.1 x 39.6	2.51	7.42	137.31	32.4	0.20	18.2
RK_28_2313.2A	87.1 x 39.1	2.55	6.97	146.21	38.3	0.24	24.2
RK_30_2321.0A	89.3 x 39.5	2.55	6.84	126.53	26.4	0.14	12.2
RK_30_2321.1B	87.2 x 39.6	2.54	7.47	157.93	25.8	0.17	12.9
RK_30_2321.7B	86.7 x 39.6	2.56	6.28	162.71	28.3	0.22	16.6
RK_30_2322.3B	89.8 x 39.6	2.53	7.51	137.97	31.5	0.23	19.2
RK_30_2322.4A	88.6 x 39.6	2.56	6.49	148.44	34.4	0.18	18.1

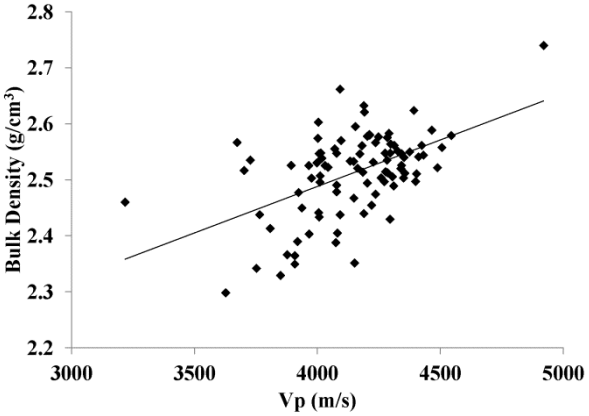

Figure 4: P-Wave velocity versus bulk density.

4.3 Uniaxial Compressive Strength and Tensile Strength

Variation in sample uniaxial compressive strength is from 75-211 MPa as seen in Figure 6 and Table 1. This indicates that although the rock type tested in this study is of similar nature, there is quite a range of variability in the ultimate strength of these specimens. This can be related to several factors. Alteration intensity of the rock specimen appears to be a very critical factor in the strength of the rocks, but is also one of the most difficult factors to quantify. As seen in the Section 4.1, the alteration intensity of the sample set is from moderate to intense alteration. It would be expected that the more altered rocks are inherently weaker. However, this does not appear to be true across the whole sample set, and therefore other parameters must be analyzed to extrapolate behavior of the sample data set.

Other quantifiable parameters such as porosity, density, and acoustic velocities show a good correlation to UCS. This can be attributed to several factors; density of the samples increases the sonic velocity and also shows a decrease in porosity. Therefore, we see stronger specimens with lower porosity and higher density values (Figure 5). Also, there appears to be a good correlation between compressional acoustic velocity and UCS (Figure 7), showing that specimens with higher compressional wave velocity also have higher strength.

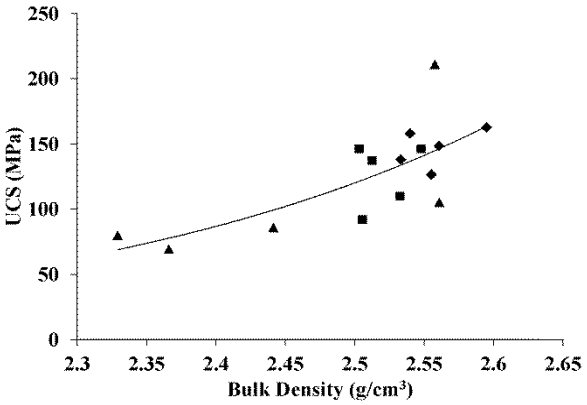

Figure 5: Bulk density versus UCS.

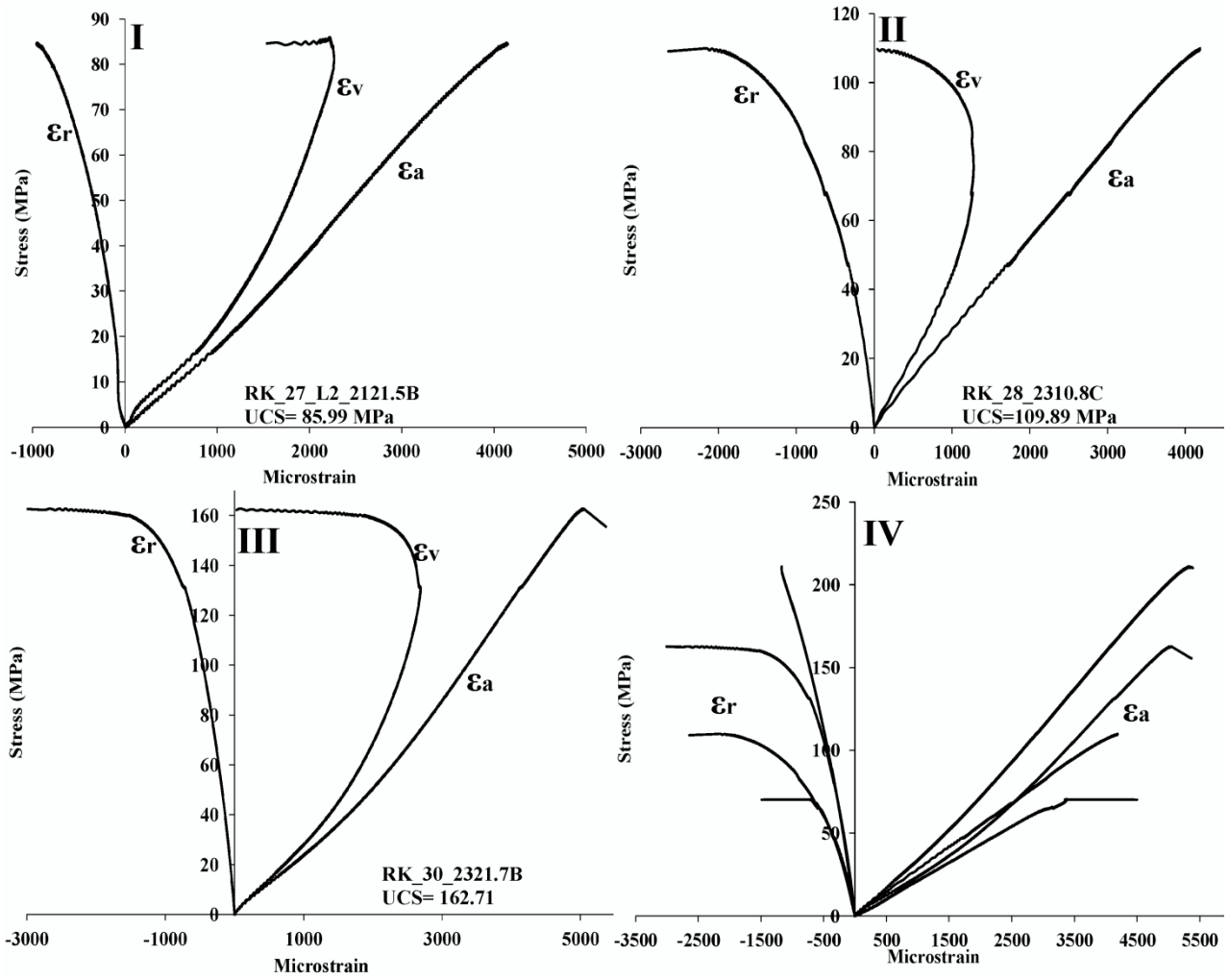

Figure 6: Stress-Strain Curves for representative specimens within sample dataset. εa is axial deformation, εv is volumetric deformation and εr is radial deformation. Reversal of strain in Plot II at 45 MPa and 68 MPa and Plot III at 130 MPa are present and are the result of irregularities within the sample. Plot IV is representative of the range of strength and deformation observed within the dataset analyzed, with volumetric strain omitted for clarity.

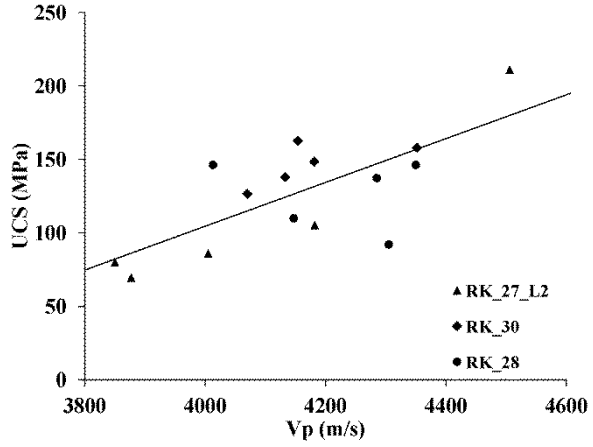

Figure 7. P-wave velocity versus UCS.

Further analysis of the stress-strain curves (Figure 6) reveals that the materials show non-linear deformation and occasional deflections in the datasets. We observe that these 'steps' in the stress-strain curves result in a volumetric increase in the sample. These can be attributed to slip within the sample before ultimate failure. This slip is likely due to high deformation along microfractures and vugs, and phenocryst failures within the samples that did not result in total yield of the sample.

Table 2: Brazilian Indirect Tensile Testing Results

Parameter	Minimum	Maximum	Mean
Diameter (mm)	24.6	28.5	27.2
Thickness (mm)	53.51	53.87	53.72
Mass (g)	145.8	176.4	162.02
Density (g/cm^3)	2.41	2.72	2.54
Porosity (%)	3.4	12.6	8.7
Tensile Strength (MPa)	9.99	24.13	15.39
UCS (MPa)	69.53	211.05	127.8
Tensile/UCS	7.6%	16.5%	12.7%

Rocks fail under tensile stresses much earlier and at lower loads than when loaded under compressional stresses (Vishal et. al, 2011). Therefore, for drilling and wellbore completion, tensile strength is very important for determining the load that subsurface rocks can handle before tensile fractures begin to propagate. Tensile fractures can cause problems during drilling and cementing, acting as lost circulation zones. Also, tensile fractures can be used to determine the orientation of principal stresses in the subsurface, and by knowing the tensile strength of these rocks, magnitude of these stresses can be inferred (Peska and Zoback, 1995 and Zoback et al, 2003). We observe that apparent tensile strength of the samples ranges from 6-14% of uniaxial compressive strength. Rajabzadeh et al. (2012) showed a similar ratio in a study of both sedimentary and metamorphic carbonate rocks that showed tensile strength to be on the order of 7-19% of UCS. These data will be utilized in further studies to determine stress magnitude and orientation within the Rotokawa reservoir (Davidson et al., this volume).

5. CONCLUSION

We have presented our initial studies of the physical properties of the Rotokawa Andesite and correlation to mechanical properties. During our testing we have observed that there is a large variability in physical, mechanical and acoustic properties of the reservoir rock. From these findings, we infer that both alteration within the material and presence of microfractures strongly influence all of the studied properties.

Tensile strength is shown to be on average, 12% of the compressive strength of the andesites. This is an important finding as tensile failure appears to be ubiquitous within wells at the Rotokawa field. By exploiting this weakness in reservoir rocks, it is possible that tensile fractures may be exploited to enhance low permeability wells.

The determination of physical and mechanical properties presented within this study also provides data that can be used in further modeling of the Rotokawa geothermal field. In planning future drilling, stimulation and modeling of stress states of the Rotokawa reservoir, these data can be used as real-world values to optimize future developments of the field.

In addition to the presented data, several other datasets are being pursued at UC including more advanced triaxial deformation studies, thermal property studies and permeability studies. Additionally, the role of thermal and mechanical stressing will be emphasized with respect to tensile failures. These additional datasets will provide further insight into the behavior and properties of the Rotokawa Andesite and help to fully refine the existing models for the dynamics of the reservoir.

ACKNOWLEDGEMENTS

The authors would like to thank Mighty River Power Ltd. for support and funding of this study as well as the Rotokawa Joint Venture for providing the samples used in this study. Staff of GNS Science, Wairakei Research Centre have also been very helpful and provided open dialogue of results and discussions relating to the parameters presented in this study. Additionally, the staff of the Department of Geological Sciences at the University of Canterbury have been invaluable in providing assistance with data collection and reporting provided in this study.

REFERENCES

ASTM. D 7012 – 10 Standard Method for Compressive Strength and Elastic Moduli of Intact Rock Core Specimens under Varying States of Stress and Temperatures. Annual Book of Standards, Vol. 04.09. (2007)

Barton, C.A., Zoback, M.D., Moos, D. Fluid flow along potentially active faults in crystalline rock. *Geology*. Vol. 23. No 8. pp. 683-686. (1995).

Hickman, S., Zoback, M.D., Benoit, R. Tectonic controls on fault-zone permeability in a geothermal reservoir at Dixie Valley, Nevada. *Rock Mechanics in Petroleum Engineering*. Vol 1. Pp. 79-86. (1998)

Horie, T., Muto, T. The World's Largest Single Cylinder Geothermal Power Generation Unit- Nga Awa Purua Geothermal Power Station, New Zealand. *GRC Transactions.* Volume 34. Pp. 1039-1044. (2010).

Kilic, R. A unified alteration index (UAI) for mafic rocks. *Environmental and Engineering Geoscience*. November, 1999. Vol. 5. No. 4. pp. 475-483 (1999).

Krupp, R.E. and Seward, T.M. The Rotokawa geothermal system, New Zealand : an active epithermal gold-depositing environment. *Economic Geology and Bulletin of the Society of Economic Geologists.* Vol. 82. No. 5. Pp. 1109-1129. (1987).

Lebedev, A. V., V. V. Bredikhin, I. A. Soustova, A. M. Sutin, K. Kusunose. Resonant acoustic spectroscopy of microfracture in a Westerly granite sample, *Journal of Geophysical Research.* Vol. 108. No. B10. (2003).

Legman, H., Sullivan, P. The 30 MW Rotokawa I Geothermal Project: Five Years of Operation. *International Geothermal Conference, 2003*, Reykjavik, Iceland. Paper 068. Pp. 26-31. (2003).

Maji. A.K. Review of noninvasive techniques for detecting microfracture. *Advanced Cement Based Materials.* Vol. 2. Issue 5. pp. 201-209. (1995)

Peska, P. Zoback, M.D. Compressive and tensile failure of inclined wellbores and determination of in situ stress and rock strength. *Journal of Geophysical Research*. Vol. 100. No. B7. Pp. 12791-12811. (1995).

Pochee, A. Mass transfer and hydrothermal alteration in the Rotokawa Andesite, Rotokawa geothermal field, New Zealand. Master's Thesis. University of Auckland School of Environment. 147p. (2010).

Rae, A. Rotokawa Geology and Geophysics. *GNS Science Consultancy Report.* 2007/83. 17p. (2007).

Rae, A.J., McCoy-West, A.J., Ramirez, L.E., Alcaraz, S.A.. Geology of Production Well RK28, Rotokawa Geothermal Field, *GNS Science Consultancy Report* 2009/253. 44p. (2009).

Rae, A.J., McCoy-West, A.J., Ramirez, L.E., McNamara, D. Geology of Production Wells RK30L1 and RK30L2, Rotokawa Geothermal Field, *GNS Science Consultancy Report* 2010/02. 40p. (2010).

Rajabzadeh, M.A., Moosavinasab, Z. and Rakhshandehroo, G. Effecots of Rock Classes and Porosity on the Relation between Uniaxial Compressive Strength and Some Rock Properties for Carbonate Rocks. *Rock Mechanics and Rock Engineering.* Vol 45. Issue 1. Pp.113-122. (2012).

Ramirez, L.E., Hitchcock, D. Geology of Production Well RK27L2, Rotokawa Geothermal Field, *GNS Science Consultancy Report* 2010/100. 37p. (2010).

Ulusay R. and Hudson, J.A. The Complete ISRM Suggested Methods for Rock Characterization, Testing and Monitoring: 1974-20006. International Society for Rock Mechanics. 628p. (2007).

Vishal, V., Pradhan, S.P., Singh, T.N. Tensile strength of rock under elevated temperatures. *Geotechnical and Geological Engineering*. Vol. 29. Issue 6. Pp. 1127-1133. (2011).

Zoback, M.D., Barton, C.A., Brudy, M., Castillo, D.A., Finkbeiner, T., Grollimund, B.R., Moos, D.B., Peksa, P., Wards, C.D., Wiprut, D.J. Determination of stress orientation and magnitude in deep wells. *International Journal of Rock Mechanics and Mining Sciences.* Vol. 40. Pp. 1049-1076. (2003).